MICROSCOPIC CALCULATIONS OF β-DECAY RATES FOR r-PROCESS*

Tomislav Marketin[a], André Sieverding[b], Meng-Ru Wu[b]
Nils Paar[a], Gabriel Martínez-Pinedo[b,c]

[a]Department of Physics, Faculty of Science, University of Zagreb
10000 Zagreb, Croatia
[b]Institut für Kernphysik (Theoriezentrum), Technische Universität Darmstadt
64289 Darmstadt, Germany
[c]GSI Helmholtzzentrum für Schwerionenforschung
Planckstraße 1, 64291 Darmstadt, Germany

(Received January 17, 2017)

Elements heavier than iron are being created in massive, explosive astrophysical scenarios such as core-collapse supernovae and neutron star mergers. Heavy element nucleosynthesis is a very complex process that requires the knowledge of the properties, mainly nuclear masses, neutron capture and beta-decay rates, of thousands of nuclei. However, due to the limitations of current experimental facilities, only a relatively small number of nuclei have so far been studied experimentally. Given the amount of nuclei, and the regions of the nuclear chart involved in the heavy element nucleosynthesis, it is necessary to use models that can be reliably applied to even the most exotic nuclei. Thus, the use of microscopic nuclear structure models presents itself as the logical choice, because the underlying microscopic theory of nuclear interaction is expected to be valid across the whole nuclear chart. In this manuscript, we present the results of a large-scale calculation of β-decay rates using a fully self-consistent theoretical framework based on the relativistic nuclear energy density functional. Taking into account the first-forbidden transitions, we are able to determine the regions of the nuclear chart where these transitions are critical for the description of the decay rates. Finally, we examine the β-delayed neutron emission in all neutron-rich nuclei, from the valley of stability to the limits of nuclear binding. The results of the study are applied in an r-process simulations where we obtain an improved description of the r-process abundance pattern.

DOI:10.5506/APhysPolB.48.641

* Presented at the Zakopane Conference on Nuclear Physics "Extremes of the Nuclear Landscape", Zakopane, Poland, August 28–September 4, 2016.

1. Introduction

One of the most important open questions in nuclear astrophysics concerns the synthesis of elements heavier than iron in explosive astrophysical scenarios. The creation of approximately half of all elements heavier than iron is via the rapid neutron capture process (r-process) that is characterized by fast neutron captures in a neutron-rich environment. The path of the r-process runs very close to the neutron drip-line, from where the nuclei decay towards the valley of stability after the neutron flux diminishes. The basic mechanism of the r-process was already described in the seminal study by Burbidge *et al.* [1].

The actual site of the r-process is under discussion, with the candidates being core-collapse supernovae and neutron star mergers. Nevertheless, it is generally accepted that it occurs in explosive environments involving relatively high temperatures (up to 1 GK) and neutron densities ($n_n > 10^{20}$ g cm^{-3}). Apart from the complexities involved in simulating the astrophysical environment, the r-process presents a particularly difficult challenge due to the large amount of required input. To properly account for all the relevant reactions and processes that take place during nucleosynthesis, knowledge of a variety of nuclear properties is necessary.

Of those, β-decay properties of unstable neutron-rich nuclei critically affect the distribution of elemental abundances as they determine the speed of the flow of matter towards higher atomic numbers, thus setting the time scale of the r-process [2, 3]. Of particular importance are nuclides around the closed neutron shells at $N = 50$, 82 and 126. These nuclei display relatively low neutron capture cross sections, thus accumulating matter which results with the observed peaks in the solar system r-process distribution. Because of the practical difficulties involved in the synthesis and measurement of the properties of these nuclei, there is relatively little data available for $N = 50$ [4–7] and $N = 82$ [8–10], with no data available for $N = 126$. Therefore, the r-process simulations must rely on theoretical models for input.

There are few theoretical frameworks capable of providing all the required nuclear properties. While the interacting shell model is able to provide a detailed description of the low-energy part of the transition strength function, due to the high computational cost, it can only be applied to nuclei close to the closed shells. Because of this restriction, most of the nuclear input for astrophysical applications is obtained with semiempirical models or models based on the density functional theory. In fact, the commonly used table of β-decay half-lives has been calculated with a microscopic–macroscopic model based on a quasiparticle random phase approximation (QRPA) calculation with a schematic interaction on top of the finite range droplet model (FRDM) [11, 12].

In neutron-rich nuclei, due to the Coulomb interaction of the additional proton in the daughter nucleus, the isobaric analogue of the parent ground state is shifted to higher energies beyond the Q_β-window. Therefore, the r-process nuclei typically decay by the Gamow–Teller transitions. However, in very neutron-rich nuclei, it is often the case that the excess neutrons occupy states in one shell higher than the protons. In that case, it becomes possible for the parity changing first-forbidden transitions to provide a significant contribution to the total decay rate. In the FRDM calculations, the first-forbidden transitions have been treated separately from the allowed transitions, using the statistical gross theory.

After decay, the daughter nucleus is typically found in an excited state, from which, depending on the excitation energy, it can de-excite in different ways. β-delayed neutron emission occurs if the daughter nucleus is excited beyond the neutron separation energy S_n, as it becomes energetically possible to de-excite by neutron emission. These delayed neutrons play a critical role in the late phases of the r-process when they can contribute a significant portion of the neutron flux which shifts the matter towards higher masses [13].

In this study, we present the results of a large scale calculation of β-decay properties of neutron-rich nuclei involved in heavy element nucleosynthesis [14]. A fully self-consistent theoretical framework is utilized based on the relativistic Hartree–Bogoliubov (RHB) model [15] for the description of the ground state of open- and closed-shell nuclei, with the proton–neutron relativistic quasiparticle random phase approximation (pn-RQRPA) for the description of nuclear excitations. The residual interaction at the RQRPA level is derived from the same relativistic nuclear energy density functional (RNEDF) as was used for the ground state calculations to ensure consistency of the results for different nuclear properties.

This approach was already successfully used in studies of Gamow–Teller and higher order resonances [16, 17], β-decay half-lives of specific isotopic chains [18, 19], and stellar weak-interaction processes [20, 21]. Because of the microscopic nature of the model, based on a state-of-the-art energy density functional, the quality of the description of the nuclear properties extends further away from the valley of stability. The framework enables a proper treatment of the first-forbidden transitions on an equal footing with the allowed transitions, allowing for a meaningful comparison between their respective contributions to the total decay rate. The results of the large-scale calculation will be used to determine the single- and multiple-neutron emission probabilities and compare them with available data and results of other theoretical studies.

2. Theoretical framework

The β decay is a weak-interaction process where an unstable parent nucleus decays from the ground state into an excited state (or possible into the ground state) of the daughter nucleus which has one proton more and one neutron less than the parent nucleus. During the process, an electron and an electron antineutrino are emitted

$$ {}^{A}_{Z}X_{N} \rightarrow {}^{A}_{Z+1}Y^{*}_{N-1} + e^{-} + \bar{\nu}_{e} \, . \tag{1} $$

Therefore, in order to calculate the β-decay rate, it is necessary to determine the properties of both the parent and the daughter nucleus and the transitions between them, together with the evaluation of the phase space available to the emitted leptons. To this end, we employ a fully microscopic theoretical framework based on the relativistic nuclear energy density functional. Treating the mesons as the mediators of the nuclear force, a minimal set of meson fields is constructed consisting of the effective isoscalar–scalar σ meson, the isoscalar–vector ω meson and of the isovector–vector ρ meson. These meson fields, together with the self-consistent mean-field for nucleons and the electromagnetic field and the interactions between them, construct a complete model of a nucleus. The nuclear ground state properties are described using the relativistic Hartee–Bogoliubov model (RHB) which properly describes the pairing effects in open-shell nuclei. For all the calculations, we assume spherical symmetry of the nuclear system, and adopt the D3C* parameter set [19] which has previously been shown to provide a good description of decay properties of neutron-rich nuclei.

Nuclear excitations are obtained using the proton–neutron relativistic quasiparticle random phase approximation (pn-RQRPA) formulated in the canonical single-nucleon basis of the RHB model, extended to the description of charge-exchange excitations. The RHB + pn-RQRPA theoretical framework is fully self-consistent as the same interaction is used both at the RHB and RQRPA levels. In the $T = 1$ channel of the pn-RQRPA, we use the pairing part of the Gogny force which has been carefully adjusted to the pairing properties of finite nuclei. For the $T = 0$ proton–neutron pairing interaction, we use an Ansatz of the Gogny form with the projector onto $S = 1$ and $T = 0$ states. The strength of the $T = 0$ pairing interaction has the following form [22]:

$$ V_{0} = V_{L} + \frac{V_{D}}{1 + e^{a+b(N-Z)}} \, , \tag{2} $$

where the values of the parameters are $V_L = 160$ MeV, $V_D = 15$ MeV, $a = 7.2$ and $b = -0.3$. Parameter V_L represents the lowest pairing strength, and the sum $V_L + V_D$ the saturation value for very neutron rich nuclei. In

order to treat nuclei with odd numbers of protons or neutrons, we constrain the expectation value of the particle number operator to a corresponding odd value. We obtain an *even* RHB state, where the ground-state energy differs from the ground-state energy of the true odd system by the energy of the odd quasiparticle [23]. A recent study of β-decay in neutron-rich nuclei based on the Skyrme energy density functional has successfully applied the equal filling approximation on systems with odd number of particles [24].

3. Large-scale calculation of β-decay rates of neutron-rich nuclei

The decay rate between an initial state in the parent nucleus and a final state in the daughter nucleus may be described as

$$\lambda = \frac{\ln 2}{K} \int_0^{p_0} p_e^2 \left(W_0 - W\right)^2 F(Z,W) C(W) dp_e \,, \tag{3}$$

where W is the electron energy in units of electron mass, W_0 is the maximum electron energy that is equal to the total energy released in the decay, and p_e is the electron momentum in units of electron mass. We approximate the maximum electron energy with [25]

$$M_\mathrm{i} - M_\mathrm{f} \approx \lambda_n - \lambda_p + \Delta M_{nH} - E_\mathrm{QRPA} \,. \tag{4}$$

The constant K is measured in superallowed β-decays and is equal to $K = 6144 \pm 2$ s.

The shape factor $C(W)$ differs for different transitions. In the case of the allowed Gamow–Teller transitions, it is simply equal to the Gamow–Teller reduced transition probability

$$C(W) = B(\mathrm{GT}) \,. \tag{5}$$

However, in the case of first-forbidden transitions, the shape factor takes on a more complex form as it becomes dependent on energy

$$C(W) = k + kaW + kbW^{-1} + kcW^2 \,, \tag{6}$$

where the factors k, ka, kb, and kc are complex combinations of transition matrix elements as defined in [26]. Therefore, for first-forbidden transitions, the shape factor can significantly influence the decay rate but also the shape of the spectra of emitted electrons and antineutrinos.

The β-decay half-lives are obtained from the decay rate as

$$T_{1/2} = \frac{\ln 2}{\lambda} \,. \tag{7}$$

To determine the level of agreement between the calculated values and data, in Fig. 1 we plot the ratio of the calculated and experimental half-lives *versus* the experimental half-lives for nuclei with experimental half-lives shorter than 1 hour. Data are taken from the NUBASE 2012 evaluation of nuclear properties [27]. For long-lived nuclei, we observe a large spread of values due to the high sensitivity of the decay rate to the details of the low-energy transition strength. Long-lived nuclei have quite small Q-values, and a very small number of transitions is found within the Q-value. On the other hand, short-lived nuclei have large Q-values, and a large number of transitions contribute to the total decay rate with a larger portion of the total strength participating. Therefore, the description of the decay properties in short-lived nuclei is less sensitive to the details of a particular transitions which results in the characteristic shape of the plot, see also Refs. [12, 28].

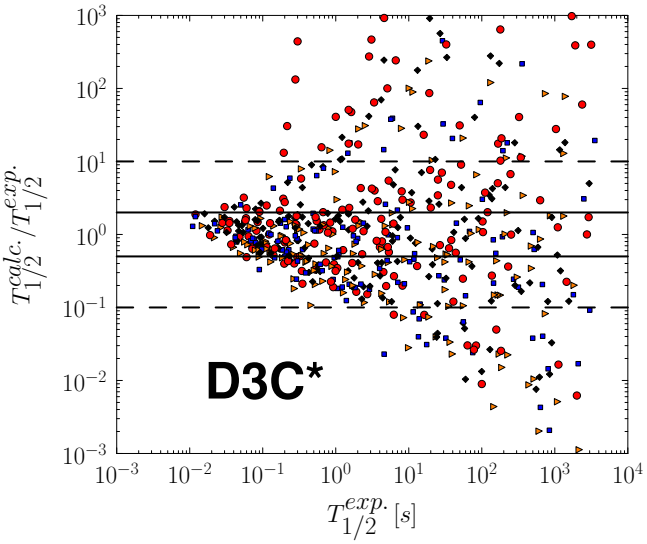

Fig. 1. (Color online) Plot of the ratio of theoretical and experimental half-lives *versus* the experimental values. Even–even nuclei are denoted with squares (blue), odd-N with triangles (orange), odd-Z with diamonds (black), and odd–odd nuclei are denoted with circles (red). Data are taken from Ref. [27].

The predictive power of the model is evident when the results are compared to data that have not been available at the time of the calculation. In a recent study, 110 half-lives have been measured, 40 of which have been measured for the first time. In Fig. 2, we compare the predicted half-lives against data of Ref. [29]. We obtain an excellent agreement with the data, within a factor of two from measurements for all isotopic chains except tin. The arch visible between neutron numbers 68 and 84 may be due to the effects of deformation which are not accounted for in this study.

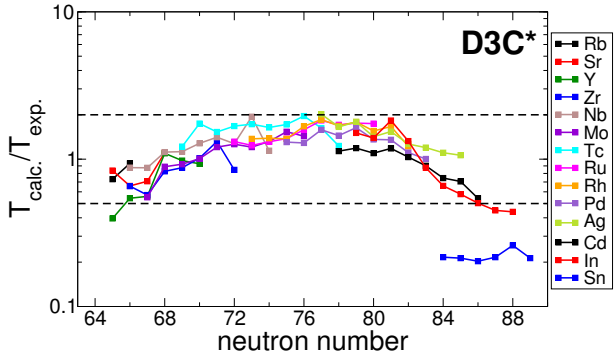

Fig. 2. Comparison of the predicted half-lives with the recent experimental results from Ref. [29]. Horizontal dashed lines indicate deviation from data by a factor of 2.

Furthermore, we can examine the impact of first-forbidden transitions on the total decay rate across the nuclear chart. In Fig. 3, we plot the contribution (in percent) of the first-forbidden transitions to the decay rate for all neutron-rich nuclei. We observe that close to the valley of stability, the first-forbidden transitions are generally not important. The protons and neutrons occupy orbits of equal parity and the decay is dominated by the Gamow–Teller transitions. Crossing the closed-neutron shells (*e.g.* $N = 50$ shell for nuclei with $20 < Z < 28$, or $N = 82$ shell for nuclei with $40 < Z < 50$), the contribution of the forbidden transitions quickly rises until it saturates at approximately 50%. Adding neutrons into the next shell enables new transitions between states with different parity and increases the contribution of the forbidden transitions. Additional neutrons continue to fill the orbits in the shell which also enables Gamow–Teller transitions between states in the same upper shell, balancing the contributions of the allowed and forbidden transitions.

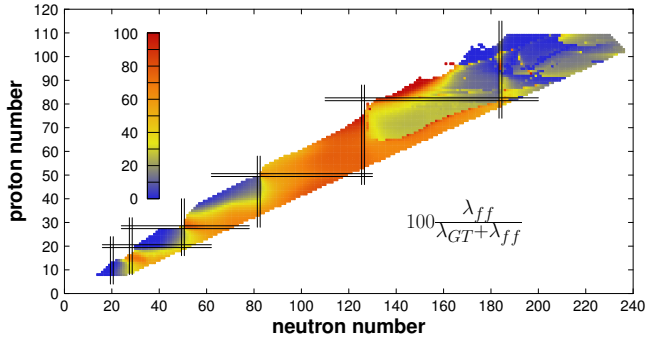

Fig. 3. Contribution of first-forbidden transitions to the total decay rate for nuclei with half-lives shorter than 1 s.

4. β-delayed neutron emission

After decaying, the daughter nucleus is typically found in an excited state. Depending on whether the excitation energy is larger than neutron separation energy, it is possible for the nucleus to de-excite by neutron emission rather than gamma emission. In nuclei far from stability, the Q-values may be larger than two-neutron separation energy S_{2n} allowing for emission of multiple neutrons. To obtain the emission probability, we use a simple approximation where we assume that the nucleus always emits as many neutrons as energetically allowed. This approximation neglects the competition between neutron and gamma emission, and systematically overestimates neutron emission probabilities.

In Fig. 4, we plot the average number of emitted neutrons for all neutron-rich nuclei,

$$\langle n \rangle = \sum_i i \, P_{in} \, . \tag{8}$$

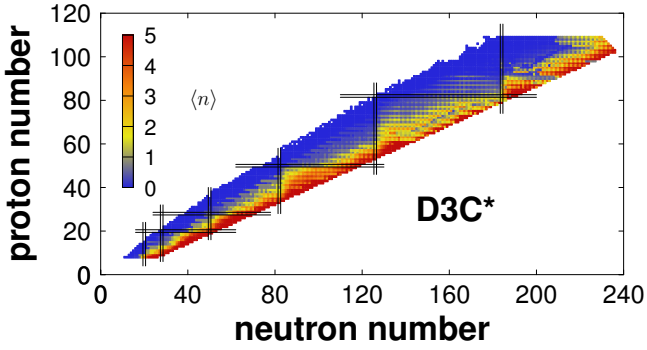

Fig. 4. Average number of neutrons emitted after β decay.

One can clearly observe the characteristic odd–even staggering of $\langle n \rangle$ with the atomic number that is a consequence of the staggering of β-decay Q-values. Weaker odd–even staggering is also visible within isotopic chains due to the staggering of the neutron separation energies.

5. Conclusion

Decay properties of neutron-rich nuclei are an important ingredient for simulations of heavy element nucleosynthesis. We have employed a fully microscopic, self-consistent theoretical framework based on the relativistic nuclear energy density functional to describe the β-decay half-lives and β-delayed neutron emission properties of neutron-rich nuclei participating in the r-process.

The results are in a very good agreement with the available data across the nuclear chart. No odd–even staggering is observed in the calculated half-lives in agreement with observations, and the average description of the half-lives is comparable to the study based on the FRDM. We were also able to describe the contribution of the first-forbidden transitions to the total decay rates, which becomes particularly important at the crossing of closed neutron shells.

This work was supported in part by the Helmholtz International Center for FAIR within the framework of the LOEWE program launched by the State of Hesse, by the Deutsche Forschungsgemeinschaft through contract No. SFB 634, the Helmholtz Association through the Nuclear Astrophysics Virtual Institute (VH-VI-417), the IAEA Research contract No. 18094/R0, the Croatian Science Foundation under the project Structure and Dynamics of Exotic Femtosystems (IP-2014-09-9159) and by the QuantiXLie Centre of Excellence.

REFERENCES

[1] E.M. Burbidge, G.R. Burbidge, W.A. Fowler, F. Hoyle, *Rev. Mod. Phys.* **29**, 547 (1957).
[2] K. Langanke, G. Martínez-Pinedo, *Rev. Mod. Phys.* **75**, 819 (2003).
[3] M. Arnould, S. Goriely, K. Takahashi, *Phys. Rep.* **450**, 97 (2007).
[4] P.T. Hosmer *et al.*, *Phys. Rev. Lett.* **94**, 112501 (2005).
[5] P. Hosmer *et al.*, *Phys. Rev. C* **82**, 025806 (2010).
[6] M. Quinn *et al.*, *Phys. Rev. C* **85**, 035807 (2012).
[7] M. Madurga *et al.*, *Phys. Rev. Lett.* **109**, 112501 (2012).
[8] F. Montes *et al.*, *Phys. Rev. C* **73**, 035801 (2006).
[9] S. Nishimura *et al.*, *Phys. Rev. Lett.* **106**, 052502 (2011).
[10] B. Pfeiffer, K.L. Kratz, F.K. Thielemann, W.B. Walters, *Nucl. Phys. A* **693**, 282 (2001).
[11] P. Möller, J.R. Nix, K.-L. Kratz, *At. Data Nucl. Data Tables* **66**, 131 (1997).
[12] P. Möller, B. Pfeiffer, K.-L. Kratz, *Phys. Rev. C* **67**, 055802 (2003).
[13] A. Arcones, G. Martínez-Pinedo, *Phys. Rev. C* **83**, 045809 (2011).
[14] T. Marketin, L. Huther, G. Martínez-Pinedo, *Phys. Rev. C* **93**, 025805 (2016).
[15] D. Vretenar, A. Afanasjev, G. Lalazissis, P. Ring, *Phys. Rep.* **409**, 101 (2005).
[16] N. Paar, T. Nikšić, D. Vretenar, P. Ring, *Phys. Rev. C* **69**, 054303 (2004).

[17] T. Marketin, G. Martínez-Pinedo, N. Paar, D. Vretenar, *Phys. Rev. C* **85**, 054313 (2012).
[18] T. Nikšić *et al.*, *Phys. Rev. C* **71**, 014308 (2005).
[19] T. Marketin, D. Vretenar, P. Ring, *Phys. Rev. C* **75**, 024304 (2007).
[20] N. Paar, D. Vretenar, T. Marketin, P. Ring, *Phys. Rev. C* **77**, 024608 (2008).
[21] Y.F. Niu, N. Paar, D. Vretenar, J. Meng, *Phys. Rev. C* **83**, 045807 (2011).
[22] Z.M. Niu *et al.*, *Phys. Lett. B* **723**, 172 (2013).
[23] T. Duguet, P. Bonche, P.-H. Heenen, J. Meyer, *Phys. Rev. C* **65**, 014310 (2001).
[24] T. Shafer *et al.*, *Phys. Rev. C* **94**, 055802 (2016) [arXiv:1606.05909 [nucl-th]].
[25] J. Engel *et al.*, *Phys. Rev. C* **60**, 014302 (1999).
[26] H. Behrens, W. Bühring, *Nucl. Phys. A* **162**, 111 (1971).
[27] G. Audi *et al.*, *Chin. Phys. C* **36**, 1157 (2012).
[28] M.T. Mustonen, J. Engel, *Phys. Rev. C* **93**, 014304 (2016).
[29] G. Lorusso *et al.*, *Phys. Rev. Lett.* **114**, 192501 (2015).